Electronic supplementary information

From dinuclear to two-dimensional Dy(III) complexes: Single crystal-single crystal transformation and single-molecule magnetic behavior

Yi-Shu Jin,[a] Ke Yu,[a] Nan Zhang,[a] Yi-Quan Zhang,*[b] Cai-Ming Liu [c] and Hui-Zhong Kou*[a]

---

[a] Department of Chemistry, Tsinghua University, Beijing 100084, P. R. China. Email: kouhz@mail.tsinghua.edu.cn

[b] Jiangsu Key Lab for NSLSCS, School of Physical Science and Technology. Nanjing Normal University. Nanjing 210023, P. R. China. Email: zhangyiquan@njnu.edu.cn

[c] Beijing National Laboratory for Molecular Sciences, Center for Molecular Science, Institute of Chemistry, Chinese Academy of Sciences, Beijing 100190, P. R. China.
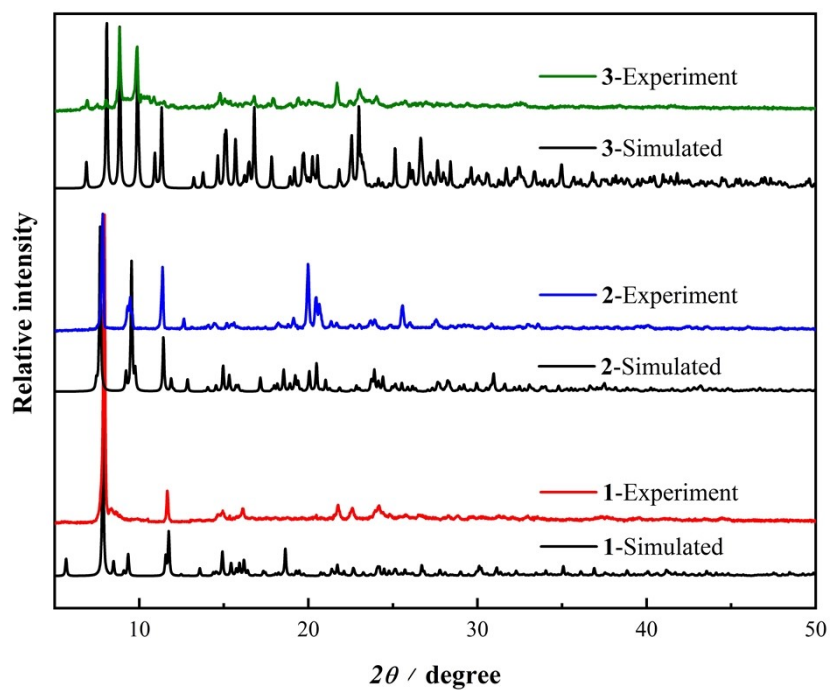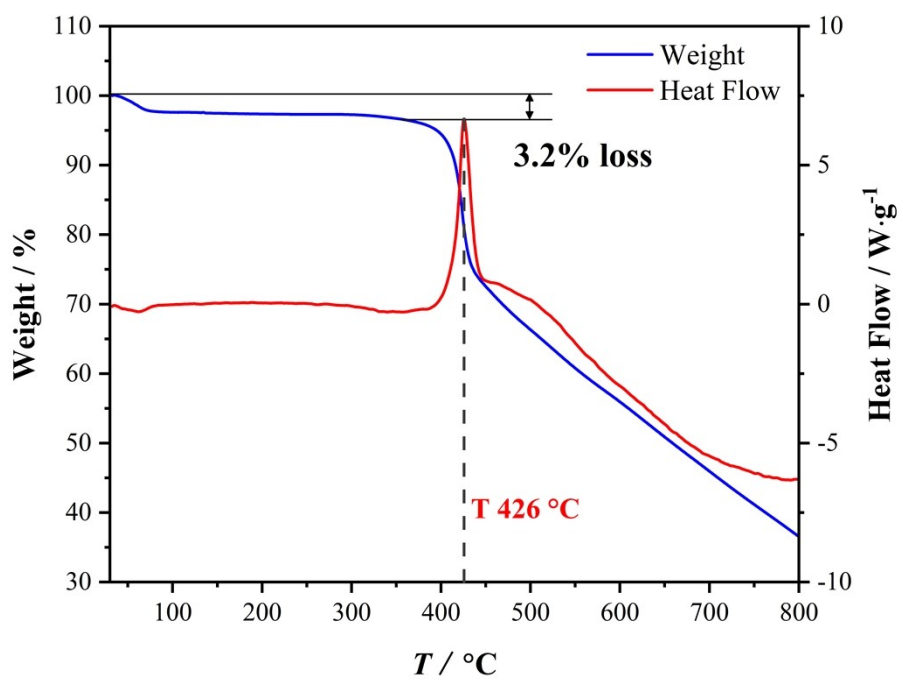
Fig. S1. Powder diffraction spectra of complexes **1-3**.

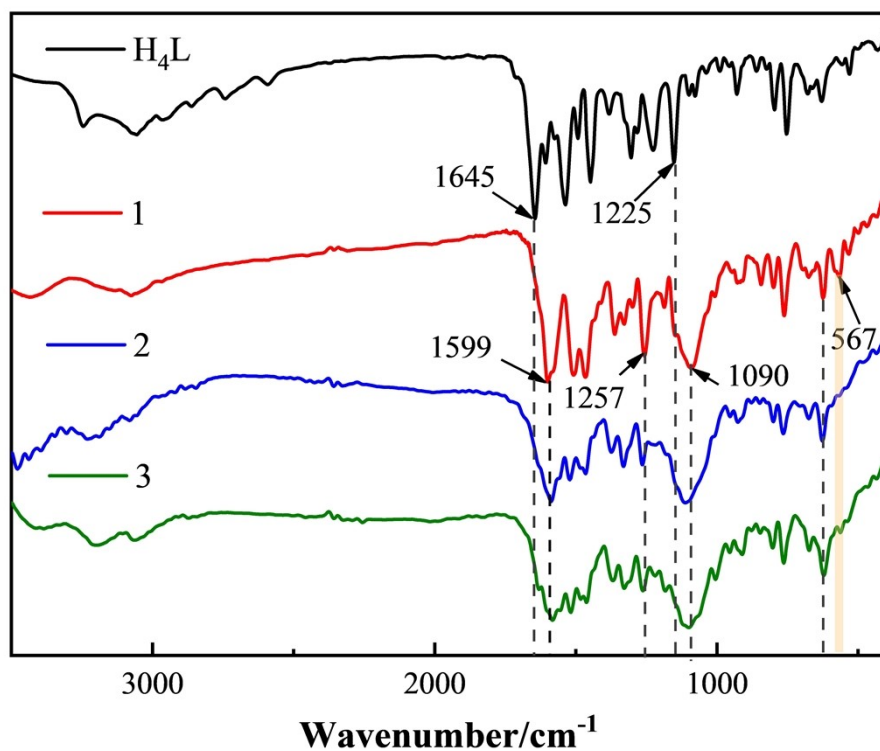**Fig. S2.** Thermogravimetric and differential thermal analysis (TGA-DSC) curves of **1**.
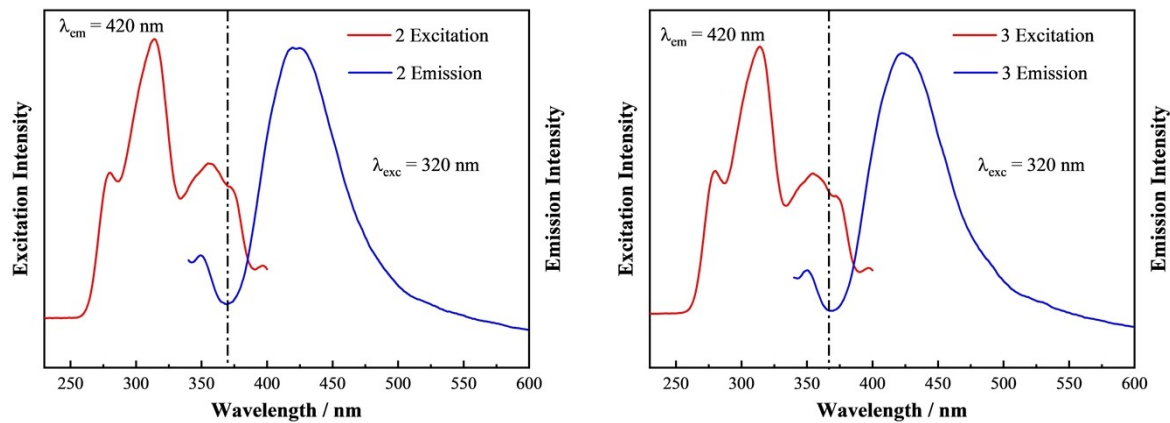
Fig. S3. IR spectra of H_4L and **1-3**.

Fig. S4. Excitation and emission spectra of **2** (left) and **3** (right) in DMF solution
$(1 \times 10^{-5}$ M).

Table S1. Crystal data and structure refinement for **1-4**.

Compound reference	1	2	3	4
Chemical formula	$C_{53}H_{44}Cl_2Dy_2N_{12}O_{19}$	$C_{58}H_{56}Cl_4Dy_2N_{14}O_{28}$	$C_{60}H_{58}Cl_4Dy_2N_{16}O_{28}$	$C_{60}H_{58}Cl_4Dy_2N_{16}O_{28}$
Formula weight	1548.90	1863.96	1918.02	1918.02
Temperature / K	173.00(10)	173.15	100.00(10)	173.00(10)
Crystal system	orthorhombic	monoclinic	triclinic	triclinic
Space group	$P2_12_12_1$	$P21/n$	P-1	P-1
a/Å	11.9057(5)	12.9807(5)	11.8821(3)	12.5478(4)
b/Å	21.5577(9)	14.8796(7)	12.2416(3)	13.1202(3)
c/Å	22.5132(13)	18.7475(9)	12.9637(3)	13.2302(4)
α/°	90	90	93.377(2)	112.328(3)
β/°	90	104.903(4)	95.040(2)	111.002(3)
γ/°	90	90	111.951(2)	97.998(2)
Volume/Å^3	5778.2(5)	3499.2(3)	1733.57(8)	1782.79(10)
Z	4	2	1	1
ρ_{calc} g/cm^3	1.780	1.769	1.837	1.786
R_{int}	0.0366	0.0491	0.0301	0.0378
GOF on F^2	1.058	1.106	1.041	1.052
R_1	0.0633	0.0911	0.0425	0.0391
wR_2	0.1591	0.2232	0.1010	0.0799
CCDC	2195447	2210188	2210189	2210190

Table S2. Selected bond distances (Å) and angels (°) for **1**.

	Dy1				Dy2		
	Distance		**Angel**		**Distance**		**Angel**
Dy1-O3	2.252(10)	O3-Dy1-O4	154.6(4)	Dy2-O1	2.435(9)	O7-Dy2-O8	152.0(4)
Dy1-O4	2.213(10)	O5-Dy1-O9	136.2(4)	Dy2-O2	2.429(8)	O8-Dy2-O1W	66.3(4)
Dy1-O5	2.469(11)	O3-Dy1-O5	73.3(4)	Dy2-O7	2.261(10)	O1-Dy2-O2	64.8(3)
Dy1-O6	2.409(10)	N7-Dy1-N10	120.0(4)	Dy2-O8	2.22(1)	N1-Dy2-N3	61.7(4)
Dy1-O9	2.626(12)	N8-Dy1-N10	61.4(4)	Dy2-O1W	2.558(10)	N2-Dy2-N3	119.6(4)
Dy1-N7	2.590(13)	N7-Dy1-N8	62.4(4)	Dy2-N1	2.609(13)	N1-Dy2-N2	61.1(4)
Dy1-N8	2.552(12)			Dy2-N2	2.628(12)		
Dy1-N9	2.531(11)			Dy2-N3	2.584(10)		
Dy1-N10	2.577(10)			Dy2-N4	2.581(9)		

Table S3. Selected bond distances (Å) and angels (°) for **2-4**.

2		3		4	
Distance and Angel					
Dy-O1	2.427(8)	Dy-O1	2.429(3)	Dy-O1	2.407(2)
Dy-O2	2.483(7)	Dy-O2	2.465(3)	Dy-O2	2.473(3)
Dy-O3	**2.175(8)**	**Dy-O3**	**2.190(3)**	**Dy-O3**	**2.215(3)**
Dy-O5	2.381(13)	Dy-O5	2.408(4)	Dy-O5	2.405(3)
Dy-N1	2.605(8)	Dy-N1	2.618(4)	Dy-O6	2.391(3)
Dy-N2	2.600(9)	Dy-N2	2.584(4)	Dy-N1	2.577(3)
Dy-N3	2.545(8)	Dy-N3	2.544(4)	Dy-N2	2.564(3)
Dy-N4	2.572(8)	Dy-N4	2.584(4)	Dy-N3	2.535(3)
Dy-N7	2.458(10)	Dy-N7	2.444(4)	Dy-N4	2.600(3)
O3-Dy-O5	146.1(4)	O3-Dy-O5	145.59(15)	O3-Dy-O5	143.54(10)
N3-Dy-N4	159.2(3)	O3-Dy-N7	143.51(14)	O3-Dy-O6	147.61(11)
N1-Dy-O2	154.2(3)	N1-Dy-O2	153.38(11)	N1-Dy-O2	150.62(10)
N2-Dy-O1	166.4(3)	N2-Dy-O1	162.52(12)	N2-Dy-O1	162.97(10)
N7-Dy-O3	143.9(3)	N7-Dy-O3	143.51(14)	N3-Dy-N4	160.61(11)

Table S4. The coordination geometry calculated by SHAPE 2.1 for **1-3**.

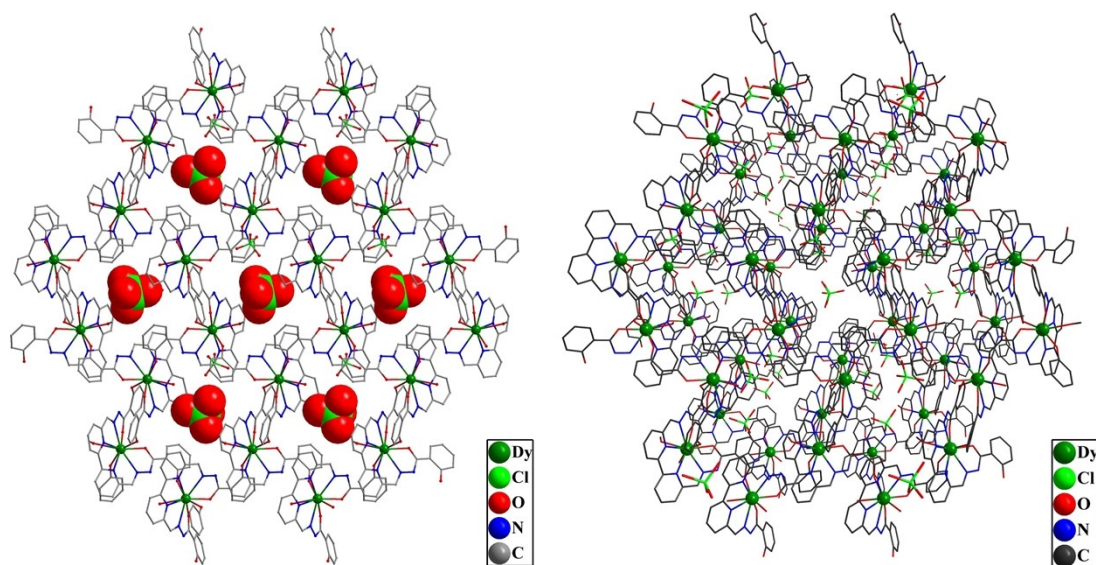| Configuration	1		2	3
	Dy1	**Dy2**	**Dy**	**Dy**
Enneagon (D9h)	33.447	32.744	29.942	31.293
Octagonal pyramid (C8v)	22.459	22.558	21.551	21.136
Heptagonal bipyramid (D7h)	13.409	13.839	14.692	15.046
Johnson triangular cupola J3 (C3v)	13.673	13.984	15.336	14.278
Capped cube J8 (C4v)	7.485	6.440	6.180	6.326
Spherical-relaxed capped cube (C4v)	6.622	5.597	5.048	5.259
Capped square antiprism J10 (C4v)	5.616	6.268	6.439	5.918
Spherical capped square antiprism (C4v)	4.794	5.454	5.304	4.772
Tricapped trigonal prism J51 (D3h)	5.716	6.015	5.306	5.204
Spherical tricapped trigonal prism (D3h)	5.480	6.058	5.939	5.589
Tridiminished icosahedron J63 (C3v)	9.416	9.276	11.519	12.416
Hula-hoop (C$_{2v}$)	**3.937**	**3.264**	**3.597**	**3.879**
Muffin (Cs)	4.156	4.664	4.284	3.793

Fig. S5. The periodic nanoscale porosity of **1** filled with perchlorate anion (left); Schematic view of the 2D network of **1** along *c* axis.
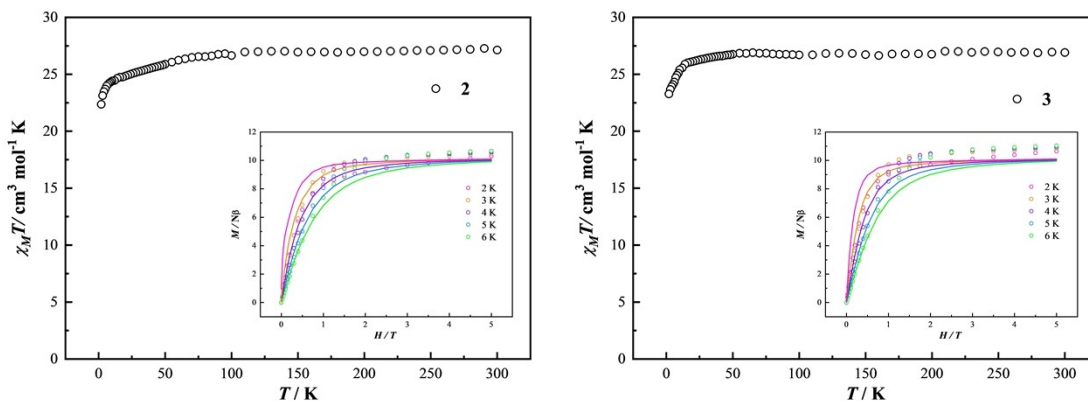
Fig. S6. Temperature dependence of $\chi_M T$ for **2** (left) and **3** (right). Inset: Experimental (circle dots) and calculated data (solid lines) of *M vs H* for **2** and **3**.
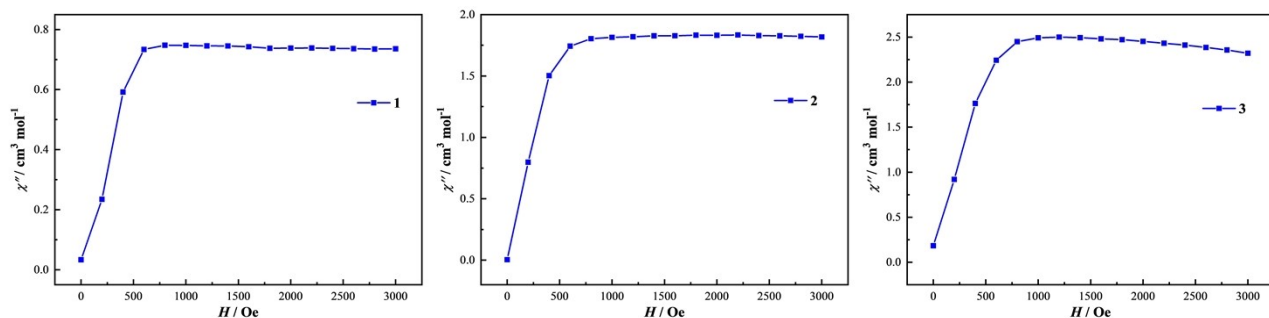

Fig. S7. Field-dependence of out-of-phase signals for **1-3** on varied dc fields at 10 K and 997Hz.
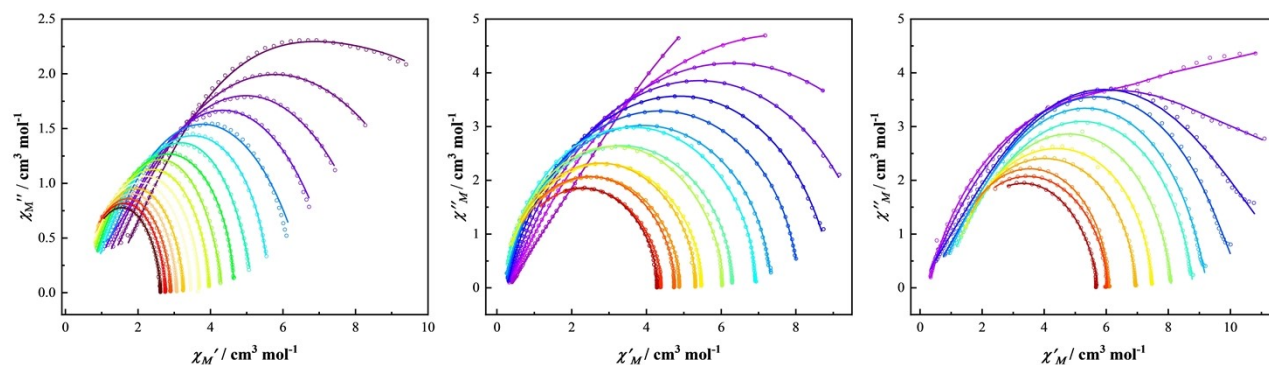

Fig. S8. Cole-Cole circle plots for **1** and **2** from 2.0 to 10.0 K, **3** from 2.0 to 8.0 K. The lines correspond to the best fitting according to the modified Debye functions.

Table S5. Linear combination of two modified Debye model fitting parameters from 2.0 K to 10 K under 800 Oe dc field for **1**.

T (K)	τ_1 (s)	α_1	τ_2 (s)	α_2	χ_0 (cm·mol^{-1})	χ_1 (cm·mol^{-1})	χ_2 (cm·mol^{-1})
2.0	0.10725	0.04229	0.00997	0.24499	1.10709	13.1478	14.94503
2.5	0.02158	0.51667	0.0007623	0.20689	0.91719	10.98869	10.74988
3.0	0.0178	0.43568	0.0003596	0.39967	0.86618	8.30736	8.79262
3.5	0.01288	0.38826	0.0001789	0.08035	0.79918	7.16485	7.54844
4.0	0.00851	0.37982	0.0001021	2.28907	0.88923	6.69972	6.48337
4.5	0.01141	0.43686	0.08225	0.25075	0.63451	7.92634	5.93653
5.0	0.00639	0.18629	0.0009591	0.3578	0.61218	3.40055	5.17761
5.5	0.00399	0.36754	0.04372	0.26753	0.5696	5.70754	4.71221
6.0	0.0027	0.1964	0.000278	0.17467	0.59263	3.6633	4.33668
6.5	0.00243	0.354	0.00882	0.36442	0.46263	6.15702	3.97082
7.0	0.00126	0.3102	0.02423	1.79341	0.05564	3.70712	4.11584
7.5	0.00101	0.3166	0.00979	0.31529	0.40852	4.09033	3.46404
8.0	0.0007624	0.30528	0.00522	0.36535	0.399	3.92221	3.24296
8.5	0.0006413	0.318	0.00286	0.36385	0.35188	4.1017	3.06194
9.0	0.0004377	0.29396	0.00338	0.36051	0.35453	3.39349	2.89635
9.5	0.0003869	0.32349	0.00171	0.37146	0.2816	3.73201	2.74923
10	0.0002653	0.27219	0.0033	0.32701	0.36038	2.88797	2.61996

Table S6. Linear combination of two modified Debye model fitting parameters from 2.0 K to 10 K under 1000 Oe dc field for **2**.

T (K)	τ_s (s)	τ_f (s)	α_s	α_f	β (cm·mol^{-1})	χ_t (cm·mol^{-1})	χ_s (cm·mol^{-1})
2.0	3.44444	0.43827	0.10296	0.42776	0.7688	18.3766	0.33603
3.0	1.1893	0.19005	0.2429	0.60606	0.90466	14.93235	0.16913
3.5	0.45967	1.74856	0.1743	0.62412	0.77032	13.0486	0.16913
4.0	0.22488	0.13949	0.08243	0.32391	0.66525	10.21186	0.26448
4.5	0.13137	0.08154	1.25304E-4	0.19543	0.36407	9.03469	0.26726
5.0	0.06159	0.30695	0.14727	0.0478	1.09309	8.16792	0.23352
5.5	0.03391	0.21022	0.13343	0.05571	1.06564	7.38257	0.20136
6.0	0.01307	0.13896	0.0929	2.08909	0.97603	7.12063	2.59313E-15
6.5	0.01232	0.12164	0.11585	0.07699	1.04217	6.31566	0.15558
7.0	0.00555	0.10553	0.07669	5.9531	0.98919	6.10504	0.09502
7.5	0.00528	0.08945	0.10758	2.08219	0.97809	5.60868	6.95932E-16
8.0	0.00274	0.04108	0.08426	1.97965	0.97906	5.42942	9.33083E-15
8.5	0.00266	0.0319	0.11426	0.1651	1.04237	4.88252	0.094
9.0	0.00149	0.0203	0.08294	1.87299	0.97501	4.8651	7.9705E-15
9.5	0.00144	0.02578	0.10483	1.83682	0.97194	4.50827	4.36123E-15
10.0	8.79197E-4	0.00655	0.08172	1.7999	0.96351	4.44759	5.30184E-16

Table S7. Linear combination of two modified Debye model fitting parameters from 2.0 K to 8.0 K under 1200 Oe dc field for **3**.

T (K)	τ_s (s)	τ_f (s)	α_s	α_f	β (cm·mol^{-1})	χ_t (cm·mol^{-1})	χ_s (cm·mol^{-1})
2.0	0.05859	3.3457	0.02674	0.39571	0.07781	27.88161	0.29858
2.5	0.09306	1.31682	0.24756	0.0881	0.51479	16.17204	0.24628
3.0	0.08472	6.47225	0.2246	0.60569	0.3569	20.73071	1.02824E-15
3.5	0.06104	0.0773	0.00634	0.48289	0.30602	12.29853	5.85746E-17
4.0	0.03994	0.02225	0.02221	0.4598	0.48405	10.46017	0.21908
4.5	0.02505	0.01035	0.00784	0.34593	0.52637	9.28647	0.52708
5.0	0.01653	0.00503	0.03961	0.29638	0.60095	8.81349	0.72769
5.5	0.00958	0.00243	0.06494	0.21907	0.71815	8.10269	0.84028
6.0	0.0085	0.00317	1.96304E-4	0.13428	0.32601	7.48751	0.9798
6.5	0.00606	0.00217	0.00252	0.11109	0.26245	6.95481	0.98286
7.0	0.00146	0.00342	0.07698	0.00185	0.72026	6.08912	0.93062
7.5	0.00133	0.00907	0.19505	0.36252	1.12131	5.99961	0.67499
8.0	9.00024E-4	0.04668	0.1387	5.7584	0.98759	5.74152	0.83867

Computational details

Complex **1** has two magnetic center Dy^{III} ions indicated as **Dy1** and **Dy2**. For binuclear complexes **2** and **3**, we only need to calculate one individual Dy^{III} fragment (**Dy1**) due to the centrosymmetric structure (see Figs. S8 and S0). Complete-active-space self-consistent field (CASSCF) calculations on individual Dy^{III} fragments have been carried out with OpenMolcas program package. Each of individual Dy^{III} fragments for **1**–**3** was calculated keeping the experimentally determined structures of the corresponding compounds while replacing the other Dy^{III} ions with diamagnetic Lu^{III}.

The basis sets for all atoms are atomic natural orbitals from the ANO-RCC library: ANO-RCC-VTZP for Dy^{III}; VTZ for close N and O; VDZ for distant atoms. The calculations employed the second order Douglas-Kroll-Hess Hamiltonian, where scalar relativistic contractions were taken into account in the basis set and the spin-orbit couplings were handled separately in the restricted active space state interaction (RASSI-SO) procedure.[S1,S2] For each individual Dy^{III} fragment, active electrons in 7 active orbitals include all f electrons (CAS(9 in 7 for Dy^{III})) in the CASSCF calculation. To exclude all the doubts, we calculated all the roots in the active space. We have mixed the maximum number of spin-free state which was possible with our hardware (all from 21 sextets, 128 from 224 quadruplets, 130 from 490 doublets) for each fragment. SINGLE_ANISO program was used to obtain the energy levels, g tensors, magnetic axes, *et al.* based on the above CASSCF/RASSI-SO calculations.

References

S1 P. Å. Malmqvist, B. O. Roos, B. Schimmelpfennig, *Chem. Phys. Lett.,* **2002**, *357,* 230–240.
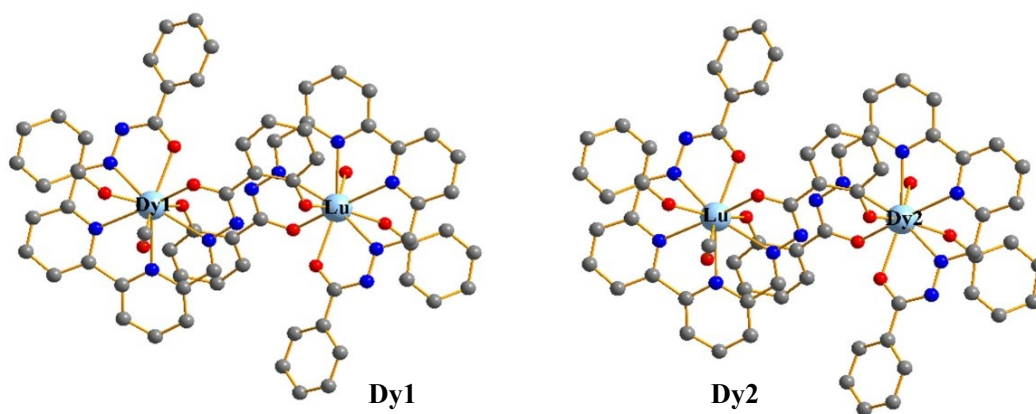S2 B. A. Heß, C. M. Marian, U. Wahlgren, O. Gropen, *Chem. Phys. Lett.,* **1996**, *251,* 365–371.

Fig. S9. Calculated model structures of individual Dy^{III} fragments in complex **1**; H atoms are omitted for clarify.
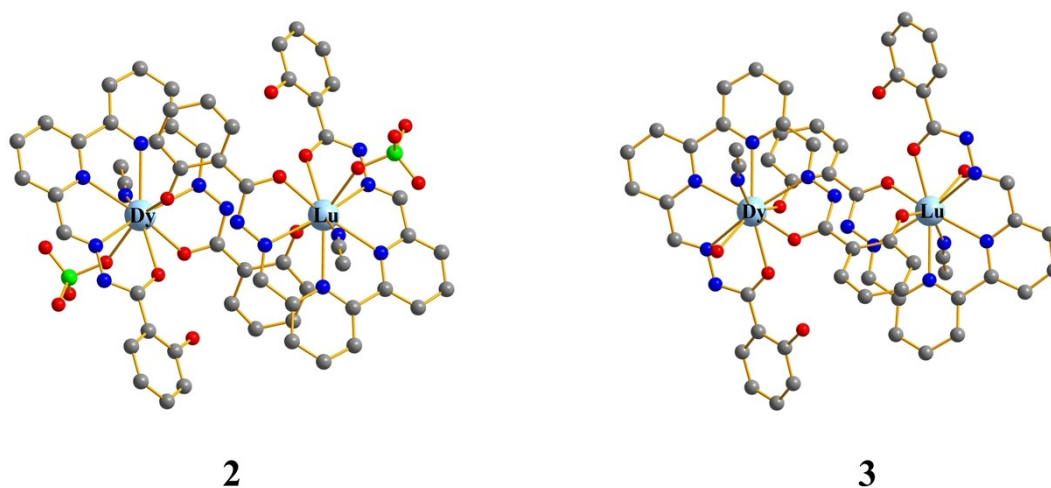

Fig. S10. Calculated model structures of individual Dy^{III} fragment in complexes **2** and **3**; H atoms are omitted for clarify.

Table S8. *Ab initio* results of the two individual Dy^{III} fragments in complex **1**.

KDs	Dy1			Dy2		
	E/cm^{-1}	*g*	m_J wave functions	E/cm^{-1}	*g*	m_J wave functions
1	0.0	0.009 0.011 19.822	99.3%|±15/2>	0.0	0.013 0.015 19.811	99.1%|±15/2>
2	272.8	0.330 0.419 16.799	96.5%|±13/2>	261.7	0.352 0.446 16.767	96.4%|±13/2>
3	468.8	1.988 3.645 11.722	75%|±11/2>+9%|±1/2>+6.7%|±7/2>	447.1	1.768 2.929 12.064	78%|±11/2>+8.7%|±1/2>+6.6%|±7/2>
4	558.5	8.213 6.709 2.754	35.9%|±9/2>+25.3%|±3/2>+16.3%|±5/2>+8.5%|±11/2>+8%|±7/2>	534.7	8.548 6.214 3.678	42.4%|±9/2>+23.9%|±3/2>+16.4%|±5/2>+8.6%|±7/2>
5	637.9	0.174 2.201 12.930	40%|±1/2>+22.8%|±7/2>+15.1%|±9/2>+11.3%|±5/2>+5.3%|±11/2>	605.7	0.492 2.803 13.721	40.2%|±1/2>+26.4%|±7/2>+14.1%|±5/2>+11.7%|±9/2>
6	698.3	0.227 3.631 14.762	38.2%|±3/2>+33.8%|±5/2>+15%|±1/2>+4.8%|±9/2>	649.0	0.304 4.146 14.957	38.1%|±3/2>+32%|±5/2>+19.5%|±1/2>+4.8%|±11/2>
7	724.0	1.380 3.516 13.766	27.6%|±9/2>+26.4%|±7/2>+25.1%|±1/2>+13.7%|±3/2>	676.4	1.124 3.763 13.240	27.8%|±9/2>+25.3%|±1/2>+22.8%|±7/2>+17.4%|±3/2>
8	828.3	0.240 0.375 17.973	32.3%|±5/2>+32.3%|±7/2>+15.2%|±3/2>+12.3%|±9/2>	771.1	0.226 0.357 17.872	32.6%|±5/2>+32.2%|±7/2>+14.9%|±3/2>+12.8%|±9/2>

Table S9. *Ab initio* results of the individual Dy^{III} fragment in complexes **2** and **3**.

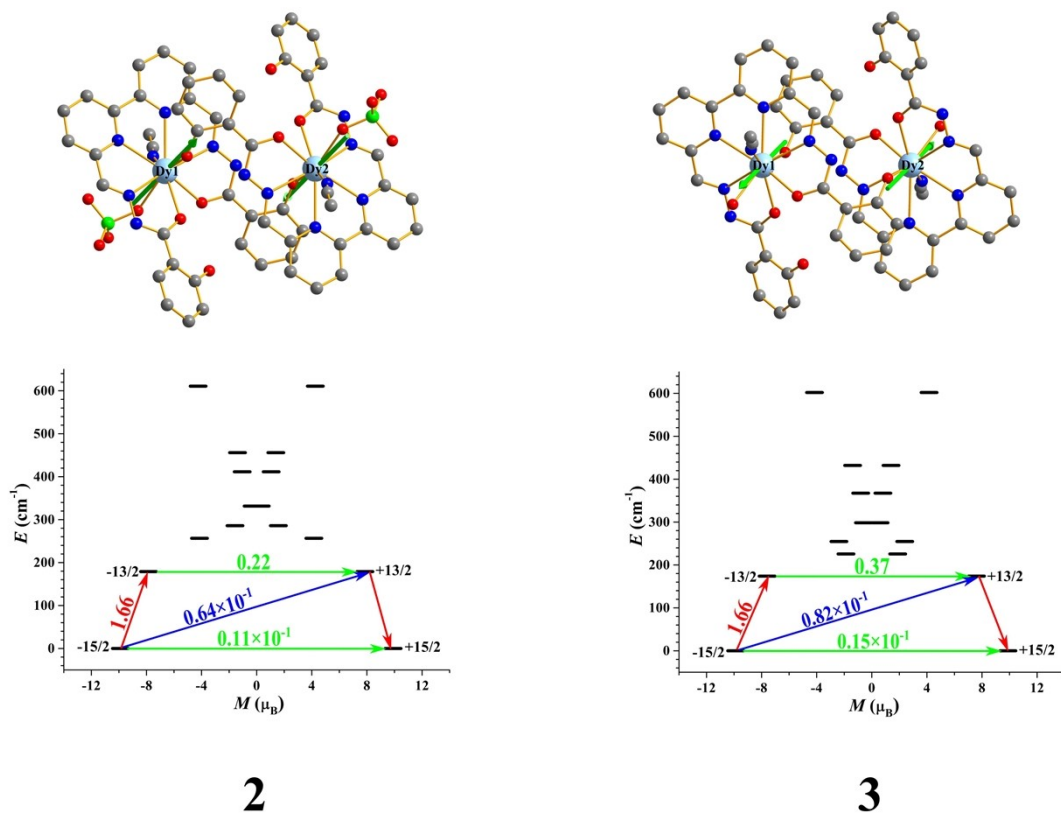| KDs	2			3		
	E/cm^{-1}	g	m_J wave functions	E/cm^{-1}	g	m_J wave functions
1	0.0	0.031 0.037 19.794	99.3%|±15/2>	0.0	0.037 0.057 19.764	99.0%|±15/2>
2	179.0	0.491 0.786 16.486	83.2%|±13/2>+8.8%|±11/2>	173.9	0.708 1.332 16.048	80.1%|±13/2>+7.9%|±11/2>+6%|±1/2>
3	256.5	2.664 5.857 10.232	33.9%|±11/2>+30.1%|±9/2>+9.1%|±3/2>+7.9%|±5/2>+7.3%|±1/2>	225.7	2.872 4.816 12.629	21%|±9/2>+20%|±11/2>+18.7%|±7/2>+17.8%|±5/2>+10.6%|±3/2>
4	285.9	0.995 3.055 11.448	41.1%|±7/2>+22.1%|±5/2>+13.7%|±9/2>+12.9%|±11/2>	254.7	1.858 3.170 12.996	28.4%|±7/2>+26.2%|±9/2>+24.4%|±11/2>+13.2%|±5/2>
5	331.6	0.500 2.480 13.106	37%|±3/2>+21.3%|±5/2>+14.2%|±11/2>+9.9%|±1/2>+7.8%|±9/2>	298.5	0.241 1.417 13.511	33.3%|±3/2>+20.8%|±5/2>+16%|±11/2>+11.8%|±1/2>+9.3%|±13/2>
6	411.4	1.639 3.000 11.545	54.9%|±1/2>+16.4%|±11/2>+10.5%|±5/2>+9.6%|±7/2>	364.7	0.729 1.463 16.015	39.5%|±1/2>+14.2%|±5/2>+14%|±11/2>+12.8%|±7/2>+10.2%|±3/2>
7	456.0	1.447 4.936 12.321	37.1%|±3/2>+20.3%|±9/2>+16.5%|±1/2>+12.9%|±5/2>+6.8%|±7/2>	432.1	0.516 0.843 16.120	30.9%|±1/2>+28.7%|±3/2>+16.8%|±9/2>+9.4%|±11/2>+7.7%|±5/2>
8	610.7	0.063 0.141 19.206	32.2%|±7/2>+24.9%|±5/2>+22.6%|±9/2>+9.5%|±3/2>	602.0	0.031 0.062 19.300	29.9%|±7/2>+25.4%|±5/2>+21.1%|±9/2>+11.8%|±3/2>+8%|±11/2>

2 **3**

Fig. S11. (top) Calculated orientations of the local main magnetic axes on Dy^{III} ions of **2** and **3** in the ground KDs. (bottom) Magnetization blocking barriers of individual Dy^{III} site of **2** and **3**. The thick black lines represent the KDs as a function of their magnetic moment along the magnetic axis. The green lines correspond to diagonal quantum tunnelling of magnetization; the blue line represents off-diagonal relaxation process. The path shown by the red arrows represents the most probable path for magnetic relaxation. The numbers at each arrow stand for the mean absolute value of the corresponding matrix element of transition magnetic moment.
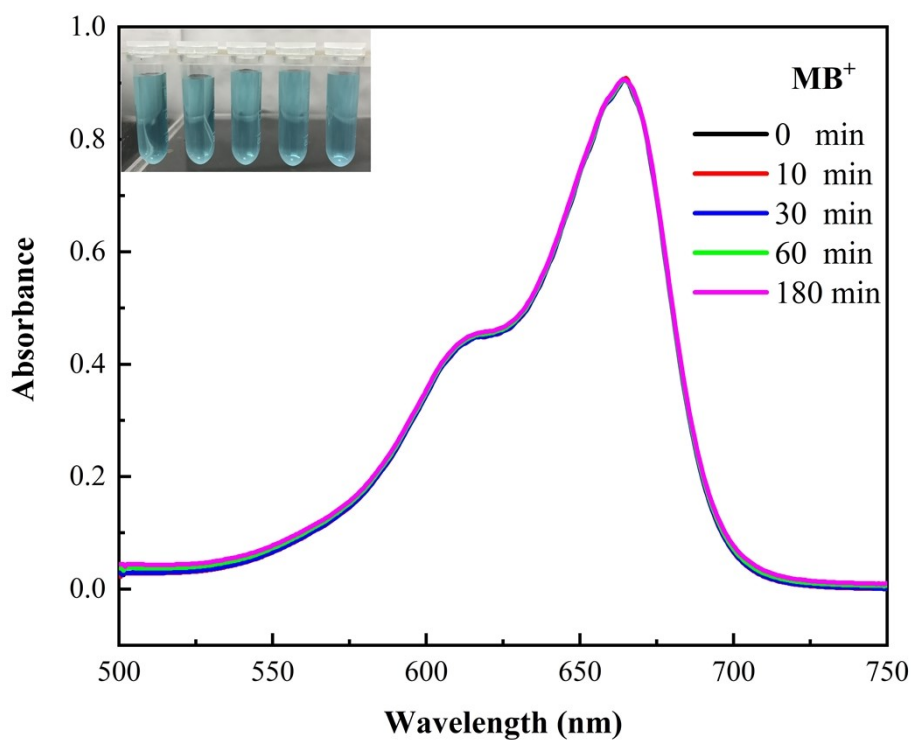
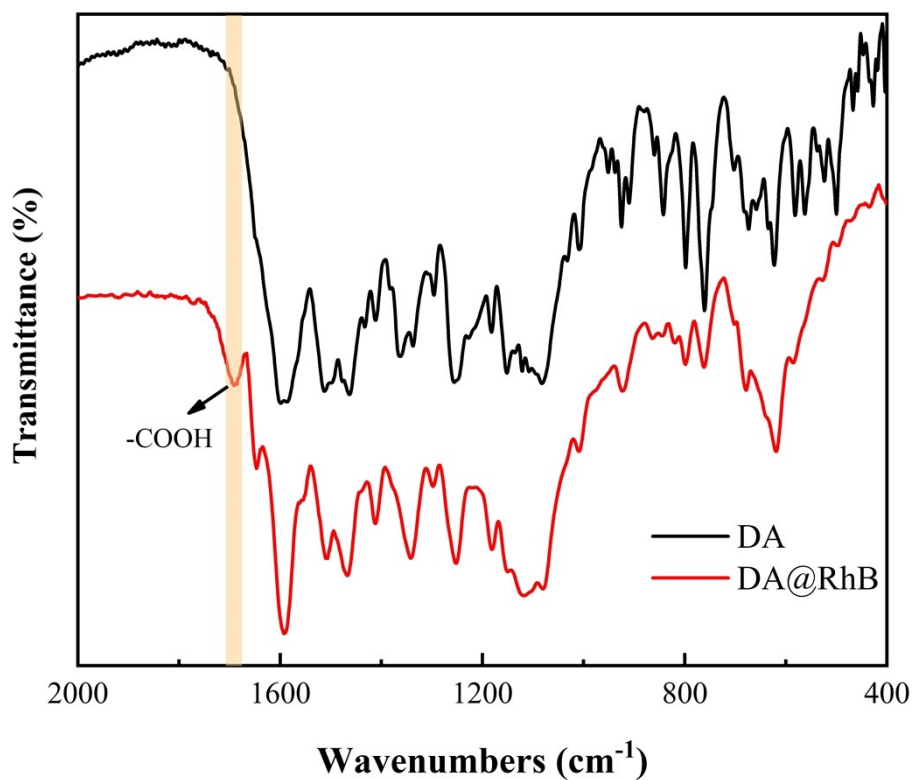**Fig. S12.** UV/vis spectra for the process of adsorption on MB$^+$.

Fig. S13. IR spectra of **1** after adsorption for RhB$^+$.

Table S10. Comparison of the magnetic properties (U_{eff}) for Dy-SMMs with a single Dy-$O_{phenoxy}$ bond

Complex	Dy-$O_{phenoxy}$/Å	U_{eff}/K	Reference
[Dy(L^R)(H_2O)$_4$(MeCN)](ClO$_4$)$_3$	2.175(3)	320	78
[Dy$^{III}_2$($L^{N6}_{R/S}$)$_2$(L3)$_2$(μ-OH)$_2$](BPh$_4$)$_2$	2.153(6), 2.186(6)	149.8	81
[Dy$_2$(H$_2$daps)$_2$(EtOH)$_2$(H$_2$O)$_2$(MeOH)$_2$](CF$_3$SO$_3$)$_2$	2.329(3)	124.7	80
2	2.175(8)	106.0	This work
3	2.190(3)	91.9	This work
[Dy(L^R)(L^A)$_2$](ClO$_4$)$_3$	2.172(4)	90	78
[Dy$_3$(μ_3-OH)(HL-1)$_3$(H$_2$O)$_3$](NO$_3$)$_2$	2.321(2), 2.287(6), 2.314(7)	40.1	79
[Dy$_3$(H$_1$daps)$_2$(H$_2$daps)(μ_3–OH)(EtOH)(H$_2$O)]	2.412(8), 2.204(10), 2.326(8)	5.3	80

Table S11. Comparison of maximum adsorption capacity (Q_m) on RhB$^+$ between previous reports and **1**.

Adsorbent	Q_m (mg·g^{-1})	Dosage (g·L^{-1})	ref
MIL-125	59.92	0.5	71
Zn/Co-ZIF-derived carbon	119.9	0.04	72
UiO-66	200.4	0.2	73
Magnesium silicate/carbon composite	244	1	74
H-UiO-66-3.8	487.8	1	75
AC-activated carbon	550.9	0.6	76
1	606	0.125	This work